EUROPEAN JOURNAL OF PURE AND APPLIED MATHEMATICS
2025, Vol. 18, Issue 4, Article Number 6750
ISSN 1307-5543 – ejpam.com
Published by New York Business Global

Analysis of Monkeypox Transmission Dynamics Incorporating Quarantine and Surface Contamination

Julito A. Puebla Jr.

Department of General Education, Caraga State University Cabadbaran Campus, 8605 Cabadbaran City, Philippines

Abstract. Monkeypox (Mpox) is a zoonotic viral disease that has re-emerged as a global health concern since 2022. In countries with limited vaccine access, non-pharmaceutical interventions such as quarantine and environmental sanitation remain the primary control strategies. However, existing models rarely integrate both measures within a single analytical framework. This study develops and analyzes a deterministic SEIQR-C model that incorporates quarantine protocols and surface contamination to examine the transmission dynamics of monkeypox. The model divides the human population into susceptible, exposed, infectious, quarantined, and recovered compartments, alongside a contaminated-surface component. Using the next generation matrix approach, the basic reproduction number (R_0) is derived, accounting for both direct and indirect transmission. Analytical results show that the disease-free equilibrium is locally and globally asymptotically stable when $R_0 < 1$, and that an endemic equilibrium exists when $R_0 > 1$. Numerical simulations confirm that increasing quarantine efficiency and cleaning or decay rates significantly reduce infection persistence, underscoring their vital roles in controlling monkeypox outbreaks in low-resource settings.

2020 Mathematics Subject Classifications: 92D30, 34D23, 37N25

Key Words and Phrases: Monkeypox, stability analysis, quarantine, surface contamination, SEIQR-C model, basic reproduction number

1. Introduction

Monkeypox (Mpox) is a viral zoonotic disease caused by the monkeypox virus (MPXV), a double-stranded DNA virus belonging to the *Orthopoxvirus* genus of the *Poxviridae* family [1]. The clinical presentation of Mpox closely resembles that of smallpox, with symptoms including fever, lymphadenopathy, and a vesiculopustular rash, though the disease is generally less severe than smallpox in terms of case fatality rates [2]. Since the first human case was identified in 1970 in the Democratic Republic of Congo, Mpox has remained endemic in Central and West African countries, with sporadic outbreaks occurring primarily through zoonotic spillover events [1, 3]. However, the 2022 outbreak

DOI: https://doi.org/10.29020/nybg.ejpam.v18i4.6750

Email address: julito.puebla@csucc.edu.ph (J. A. Puebla Jr.)

marked a pivotal moment in the epidemiology of Mpox, with sustained human-to-human transmission reported in over 100 countries, prompting the World Health Organization (WHO) to declare the outbreak a public health emergency of international concern [4].

Transmission of Mpox occurs through three primary routes: animal-to-human (zoonotic), human-to-human (direct), and indirect environmental transmission [1, 5]. Zoonotic transmission typically occurs through direct contact with infected animals or their bodily fluids, particularly from rodents and non-human primates, or through consumption of undercooked bushmeat [6]. Human-to-human transmission results from close contact with lesions, body fluids, or respiratory droplets from infected individuals [7]. More recently, environmental transmission has been recognized as an important secondary route, as MPXV remains viable on surfaces for several days after patient contact, particularly on bedding, clothing, and high-touch objects in both community and healthcare settings [8, 9]. Studies have detected viable MPXV DNA on household and hospital surfaces up to 15 days after contamination, highlighting the challenges of infection prevention in densely populated or poorly sanitized environments [9].

Although vaccines developed for smallpox, such as the Modified Vaccinia Ankara (MVA-BN), have demonstrated high protective efficacy against Mpox, immunization campaigns remain largely confined to high-income countries and target mainly high-risk populations [10]. In contrast, many low and middle-income countries, including the Philippines which reported confirmed Mpox cases beginning in 2022 do not have routine Mpox vaccination programs in place [11, 12]. In these regions, non-pharmaceutical interventions (NPIs), including case isolation, quarantine, and environmental sanitation, remain the primary tools for outbreak control [13, 14]. Recent modeling studies have underscored the importance of NPIs in mitigating Mpox transmission where vaccine coverage is limited, particularly in preventing sustained human-to-human and environmental transmission cycles [15–18].

Several recent studies have incorporated various strategies into the mathematical modeling of monkeypox transmission dynamics. For instance, Bolaji et al. [15] developed a compartmental model that integrates both quarantine and vaccination strategies, providing insights into how combined pharmaceutical and non-pharmaceutical interventions can reduce the basic reproduction number. Similarly, Hassan et al. [16] formulated a model emphasizing the role of environmental contamination by considering the indirect transmission of monkeypox via contaminated surfaces, with optimal control analysis for sanitation measures. While these models successfully captured critical facets of transmission, they either focused on vaccination-centric approaches with limited environmental dynamics [15], or addressed contaminated surfaces without integrating isolation or quarantine protocols [16]. Moreover, Ngungu et al. [13] examined non-pharmaceutical interventions based on real outbreak data but did not explicitly incorporate environmental reservoirs or structured isolation compartments. Therefore, a comparative gap remains in synthesizing both quarantine measures and surface contamination within a single unified framework, especially in the context of regions with low vaccination coverage.

In this study, an extended SEIQR-C model is developed to describe the transmission dynamics of monkeypox by integrating both quarantine and environmental surface

contamination. Earlier mathematical models have largely concentrated on direct human-to-human transmission, overlooking the combined effects of isolation measures and indirect transmission through contaminated surfaces. Incorporating quarantine and surface contamination into a single modeling framework provides a more comprehensive and realistic representation of the disease dynamics, as it captures both behavioral and environmental pathways of infection. The model further offers analytical and numerical insights into how variations in quarantine efficiency and cleaning or decay rate affect infection persistence and disease control, thereby enhancing the understanding of the mechanisms that influence the spread and management of monkeypox.

2. Model Formulation

To investigate the transmission dynamics of monkeypox, a deterministic SEIQR-C compartmental model is formulated, incorporating both direct human-to-human transmission and indirect transmission through contaminated surfaces. The SEIQR-C model that divides the total human population into five health-related classes, along with an environmental compartment representing surface contamination:

(i) Susceptible individuals (S) are at risk of acquiring monkeypox through direct contact with infectious individuals or indirect contact with contaminated surfaces in the environment.

(ii) Exposed individuals (E) who have been infected but are not yet infectious.

(iii) Infectious individuals (I) capable of transmitting the virus to others.

(iv) Quarantined individuals (Q) who have been isolated and no longer contribute to transmission.

(v) Recovered individuals (R) who have acquired permanent immunity.

(vi) Contaminated surfaces (C) such as bedding, clothing, and shared objects—serve as environmental reservoirs contributing to the indirect transmission of the monkeypox virus.

The total human population is given by $N = S + E + I + Q + R$, while C represents a non-human compartment contributing to indirect transmission. The model is based on the following assumptions:

(i) The population is replenished at a constant rate Λ, accounting for birth and immigration, and individuals are removed from all compartments through natural death at rate μ_h.

(ii) Susceptible individuals become infected either by direct contact with infectious individuals or indirectly through contact with contaminated surfaces. The force of infection is given by $\beta_h I + \beta_c C$, where β_h and β_c represent the direct and indirect

transmission rates, respectively. The force of infection is modeled using a standard mass-action form $\beta_h I + \beta_c C$, consistent with previous studies on monkeypox transmission [16, 18]. This formulation assumes proportional contact between susceptible individuals and both infectious humans and contaminated surfaces. The probability of infection increases proportionally with the number of infectious individuals and the level of environmental contamination.

(iii) Exposed individuals are infected but not infectious. They progress to the infectious compartment at rate γ, or exit due to natural death.

(iv) Infectious individuals either recover at rate γ_0, are quarantined at rate θ, or die naturally. Quarantined individuals are isolated from the population and do not contribute to new infections. They recover at rate γ_q or die naturally.

(v) Recovered individuals are assumed to gain permanent immunity and do not return to the susceptible class.

(vi) Infectious individuals shed the virus into the environment at rate α, contributing to surface contamination. The environmental viral load decays at rate μ_p due to natural inactivation or cleaning.

(vii) The model does not account for vertical transmission, re-infection, or disease importation. All transitions between compartments follow standard mass-action incidence. This assumption is supported by epidemiological evidence showing that recovered individuals develop lasting immunity and that vertical transmission of monkeypox has not been observed in humans [2, 6, 7]. Moreover, the use of a standard mass-action incidence follows previous modeling approaches [16, 18], which apply this form to maintain analytical tractability while capturing the essential transmission mechanisms.

Based on the aforementioned assumptions, Figure 1 presents the mathematical model depicting the transmission dynamics of monkeypox.

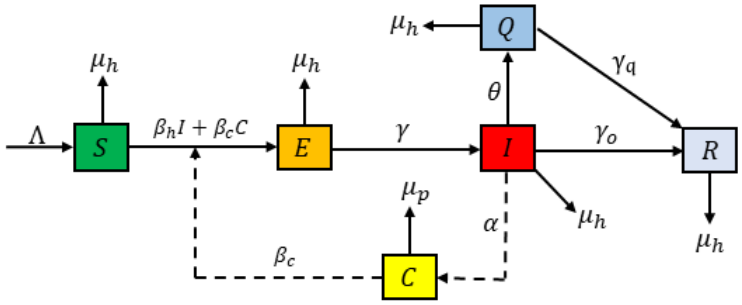

Figure 1: SEIQR-C Model for the Transmission Dynamics of Monkeypox

The transmission dynamics of the monkeypox SEIQR-C model, shown in Figure 1, are described by the following system of ordinary differential equations

$$\begin{cases} \dfrac{dS}{dt} = \Lambda - (\beta_h I + \beta_c C)\, S - \mu_h S \\ \dfrac{dE}{dt} = (\beta_h I + \beta_c C)\, S - (\gamma + \mu_h) E \\ \dfrac{dI}{dt} = \gamma E - (\gamma_0 + \theta + \mu_h) I \\ \dfrac{dQ}{dt} = \theta I - (\gamma_q + \mu_h) Q \\ \dfrac{dR}{dt} = \gamma_0 I + \gamma_q Q - \mu_h R \\ \dfrac{dC}{dt} = \alpha I - \mu_p C. \end{cases} \tag{1}$$

System (1) is defined with the following initial conditions $S(0) > 0$, $E(0) \geq 0$, $I(0) \geq 0$, $Q(0) \geq 0$, and $R \geq 0$, and $C(0) \geq 0$. All parameters in system are described in Table 1.

Parameter	Description	Value	Source
Λ	Recruitment rate of the human population	5	Assumed
β_h	Transmission rate between infectious and susceptible individuals	0.2084	[16, 17]
β_c	Transmission rate between contaminated surfaces and susceptible individuals	$7.6977\text{x}10^{-8}$	[17]
γ	Progression rate from exposed to infectious	0.2	[19]
γ_0	Recovery rate of infectious individuals	0.1490	[17, 19]
γ_q	Recovery rate of quarantined individuals	$3.5430\text{x}10^{-4}$	[17]
θ	Quarantine rate of symptomatic individuals	2	[18]
α	Contamination rate from infectious individuals to surfaces	0.004	[18]
μ_p	Cleaning or decay rate of the virus on the contaminated surfaces	1.8	Assumed
μ_h	Natural human mortality rate	0.2	[18]

Table 1: Description and Value of the Model Parameters

Theorem 1. *Given non-negative initial conditions, the solution of the SEIQR-C model (1) remains non-negative for all $t \geq 0$.*

Proof. Assume that $S(0) > 0$, $E(0) \geq 0$, $I(0) \geq 0$, $Q(0) \geq 0$, $R(0) \geq 0$, and $C(0) \geq 0$. Consider the first equation of the SEIQR-C model (1)

$$\frac{dS}{dt} = \Lambda - (\beta_h I + \beta_c C)\, S - \mu_h S. \tag{2}$$

Let $\Phi_S(t) = \beta_h I(t) + \beta_c C(t) + \mu_h$, and define the integrating factor

$$\theta_S(t) = \exp\left(\int_0^t \Phi_S(s) ds \right). \tag{3}$$

Multiply both sides by $\theta_S(t)$ and applying the Leibniz rule

$$\frac{d}{dt}\Big(\theta_S(t) S(t)\Big) = \Lambda \theta_S(t). \tag{4}$$

Integrating from 0 to t

$$\theta_S(t)S(t) = \theta_S(0)S(0) + \int_0^t \Lambda\theta_S(s)ds. \tag{5}$$

Solve for $S(t)$ yields

$$S(t) = \frac{1}{\theta_S(t)}\left(\theta_S(0)S(0) + \int_0^t \Lambda\theta_S(s)ds\right). \tag{6}$$

Since $\Lambda > 0$ and $S(0) > 0$, it implies that $S(t) \geq 0$ for all $t \geq 0$.

From the second equation of the SEIQR-C model (1), we get

$$\frac{dE}{dt} + (\gamma + \mu_h)E = (\beta_h I + \beta_c C)S. \tag{7}$$

Define the integrating factor, $\theta_E(t) = e^{(\gamma+\mu_h)t}$. Multiply both sides by $\theta_E(t)$ and applying Leibniz rule

$$\frac{d}{dt}\Big(\theta_E(t)E(t)\Big) = (\beta_h I + \beta_c C)S\theta_E(t). \tag{8}$$

Integrating from 0 to t and solve for $E(t)$, that is

$$E(t) = \frac{1}{\theta_E(t)}\left[E(0) + \int_0^t (\beta_h I(s) + \beta_c C(s))S(s)\,\theta_E(s)\,ds\right] \geq 0. \tag{9}$$

A similar method is applied to the remaining compartmental variables of the equations in the SEIQR-C model (1).

$$I(t) = \frac{1}{e^{(\gamma_0+\theta+\mu_h)t}}\left[I(0) + \int_0^t \gamma E(s)\,e^{(\gamma_0+\theta+\mu_h)s}\,ds\right] \geq 0 \tag{10}$$

$$Q(t) = \frac{1}{e^{(\gamma_q+\mu_h)t}}\left[Q(0) + \int_0^t \theta I(s)\,e^{(\gamma_q+\mu_h)s}\,ds\right] \geq 0 \tag{11}$$

$$R(t) = \frac{1}{e^{\mu_h t}}\left[R(0) + \int_0^t (\gamma_0 I(s) + \gamma_q Q(s))\,e^{\mu_h s}\,ds\right] \geq 0 \tag{12}$$

$$C(t) = \frac{1}{e^{\mu_p t}}\left[C(0) + \int_0^t \alpha I(s)\,^{\mu_p s}\,ds\right] \geq 0 \tag{13}$$

Thus, the solution of the SEIQR-C model (1) remains non-negative for all $t \geq 0$ ■

Theorem 2. *The solutions of the SEIQR-C model (1) are bounded in the region*

$$\Omega = \Big\{(S, E, I, Q, R, C) \in \mathbb{R}^6_+ : S + E + I + Q + R \leq \frac{\Lambda}{\mu_h}, \quad C \leq \frac{\alpha\Lambda}{\mu_h\mu_p}\Big\}.$$

Proof. Define the total human population as $N(t) = S(t) + E(t) + I(t) + Q(t) + R(t)$. Adding the first five equations of the SEIQR-C model gives

$$\frac{dN}{dt} = \Lambda - \mu_h N(t). \tag{14}$$

Multiplying both sides by the integrating factor $e^{\mu_h t}$ yields

$$\frac{d}{dt}\Big(N(t)e^{\mu_h t}\Big) = \Lambda e^{\mu_h t}. \tag{15}$$

Integrating both sides gives

$$N(t) = \left(N(0) - \frac{\Lambda}{\mu_h}\right) e^{-\mu_h t} + \frac{\Lambda}{\mu_h}. \tag{16}$$

Since $\mu_h > 0$, we conclude that $N(t) \leq \max\{N(0), \frac{\Lambda}{\mu_h}\}$ for all $t \geq 0$, and $\lim_{t\to\infty} N(t) = \frac{\Lambda}{\mu_h}$. Thus, the total human population is bounded.

Now consider the viral concentration on contaminated surfaces $C(t)$, which satisfies

$$\frac{dC}{dt} = \alpha I - \mu_p C. \tag{17}$$

Since $I(t) \leq N(t) \leq \Lambda/\mu_h$, we obtain

$$\frac{dC}{dt} \leq \alpha \cdot \frac{\Lambda}{\mu_h} - \mu_p C. \tag{18}$$

Multiplying by the integrating factor $e^{\mu_p t}$, we get

$$\frac{d}{dt}\left(C(t)e^{\mu_p t}\right) \leq \alpha \cdot \frac{\Lambda}{\mu_h} e^{\mu_p t}. \tag{19}$$

Solving this inequality, we find

$$C(t) \leq \left(C(0) - \frac{\alpha\Lambda}{\mu_h\mu_p}\right) e^{-\mu_p t} + \frac{\alpha\Lambda}{\mu_h\mu_p}, \tag{20}$$

and therefore,

$$\limsup_{t\to\infty} C(t) \leq \frac{\alpha\Lambda}{\mu_h\mu_p}. \tag{21}$$

Hence, all state variables of the SEIQR-C model remain bounded for all $t \geq 0$, and the solution trajectories are contained in the compact, positively invariant region

$$\Omega = \left\{(S, E, I, Q, R, C) \in \mathbb{R}^6_+ : S + E + I + Q + R \leq \frac{\Lambda}{\mu_h}, \quad C \leq \frac{\alpha\Lambda}{\mu_h\mu_p}\right\}.$$

■

3. Model Analysis

3.1. Monkeypox-Free Equilibrium and the Basic Reproduction Number

To initiate the mathematical analysis of the monkeypox model, we first identify the monkeypox-free equilibrium (MFE), also known as the disease-free equilibrium (DFE), where no infection is present in the human population and the environment. This state represents the baseline condition in which the monkeypox is absent and all individuals are either susceptible or in non-infectious compartments.

Theorem 3. *The SEIQR-C model admits a monkeypox-free equilibrium given by* $\mathcal{E}_0 = (S_0, 0, 0, 0, 0, 0)$ *where* $S_0 = \frac{\Lambda}{\mu_h}$.

Proof. Let $\mathcal{E}_0 = (S_0, E_0, I_0, Q_0, R_0, C_0)$ be a monkeypox-free equilibrium of the SEIQR-C model. To solve the MFE, we set all the time derivatives in the model to zero. That is,

$$\begin{aligned}
\Lambda - (\beta_h I_0 + \beta_c C_0)\, S_0 - \mu_h S_0 &= 0 \\
(\beta_h I_0 + \beta_c C_0)\, S_0 - (\gamma + \mu_h) E_0 &= 0 \\
\gamma E_0 - (\gamma_0 + \theta + \mu_h) I_0 &= 0 \\
\theta I_0 - (\gamma_q + \mu_h) Q_0 &= 0 \\
\gamma_0 I_0 + \gamma_q Q_0 - \mu_h R_0 &= 0 \\
\alpha I_0 - \mu_p C_0 &= 0.
\end{aligned}$$

Suppose that no infection is present in the population or the environment which means that $E_0 = I_0 = Q_0 = R_0 = C_0 = 0$. Substituting these values into the system, we obtain $S_0 = \frac{\Lambda}{\mu_h}$. Hence, the monkeypox-free equilibrium is given by

$$\mathcal{E}_0 = \Big(\frac{\Lambda}{\mu_h}, 0, 0, 0, 0, 0\Big). \tag{22}$$

■

Next, we will compute the basic reproduction number of the SEIQR-C model (1) using the next generation matrix (NGM) [20, 21]. The basic reproduction number denoted by R_0 is defined as the average number of secondary infections that occurs when one infective is introduced into a completely susceptible population [20, 21].

Now, we first identified the infected compartments contributing to the generation of new cases: the exposed individuals E, the infectious individuals I, and the contaminated surfaces C. Then, the disease transmission terms were captured in the matrix $\mathcal{F}$, representing new infections, while the transition terms between compartments were incorporated into matrix $\mathcal{V}$. These matrices are defined as

$$\mathcal{F} = \begin{bmatrix} (\beta_h I + \beta_c C)S \\ 0 \\ 0 \end{bmatrix} \quad \text{and} \quad \mathcal{V} = \begin{bmatrix} (\gamma + \mu_h)E \\ -\gamma E + (\gamma_0 + \theta + \mu_h)I \\ -\alpha I + \mu_p C \end{bmatrix}$$

The Jacobian of $\mathcal{F}$ and $\mathcal{V}$ evaluated at $\mathcal{E}_0$ are F and V, respectively.

$$F = \begin{bmatrix} 0 & \frac{\beta_h \Lambda}{\mu_h} & \frac{\beta_c \Lambda}{\mu_h} \\ 0 & 0 & 0 \\ 0 & 0 & 0 \end{bmatrix} \quad \text{and} \quad V = \begin{bmatrix} \gamma + \mu_h & 0 & 0 \\ -\gamma & \gamma_0 + \theta + \mu_h & 0 \\ 0 & -\alpha & \mu_p \end{bmatrix}$$

Then, taking the inverse of V, that is

$$V^{-1} = \begin{bmatrix} \frac{1}{\gamma+\mu_h} & 0 & 0 \\ \frac{\gamma}{(\gamma+\mu_h)(\gamma_0+\theta+\mu_h)} & \frac{1}{\gamma_0+\theta+\mu_h} & 0 \\ \frac{\alpha\gamma}{(\gamma+\mu_h)(\gamma_0+\theta+\mu_h)\mu_p} & \frac{\alpha}{(\gamma_0+\theta+\mu_h)\mu_p} & \frac{1}{\mu_p} \end{bmatrix}. \tag{23}$$

Consequently,

$$FV^{-1} = \begin{bmatrix} 0 & \frac{\beta_h \Lambda}{\mu_h} & \frac{\beta_c \Lambda}{\mu_h} \\ 0 & 0 & 0 \\ 0 & 0 & 0 \end{bmatrix} \begin{bmatrix} \frac{1}{\gamma+\mu_h} & 0 & 0 \\ \frac{\gamma}{(\gamma+\mu_h)(\gamma_0+\theta+\mu_h)} & \frac{1}{\gamma_0+\theta+\mu_h} & 0 \\ \frac{\alpha\gamma}{(\gamma+\mu_h)(\gamma_0+\theta+\mu_h)\mu_p} & \frac{\alpha}{(\gamma_0+\theta+\mu_h)\mu_p} & \frac{1}{\mu_p} \end{bmatrix} \tag{24}$$

$$= \begin{bmatrix} \frac{\Lambda\gamma(\beta_h\mu_p+\alpha\beta_c)}{\mu_h\mu_p(\gamma+\mu_h)(\gamma_0+\theta+\mu_h)} & \frac{\Lambda(\beta_h\mu_p+\alpha\beta_c)}{\mu_h\mu_p(\gamma_0+\theta+\mu_h)} & \frac{\Lambda\beta_c}{\mu_h\mu_p} \\ 0 & 0 & 0 \\ 0 & 0 & 0 \end{bmatrix} \tag{25}$$

Accordingly, the basic reproduction number of the SEIQR-C model (1) is the largest eigenvalue of FV^{-1}. Hence,

$$R_0 = \frac{\Lambda\gamma(\beta_h\mu_p + \alpha\beta_c)}{\mu_h\mu_p(\gamma + \mu_h)(\gamma_0 + \theta + \mu_h)}. \tag{26}$$

The basic reproduction number R_0 serves as a critical threshold parameter in epidemiological modeling [22]. In the SEIQR-C model, R_0 captures both direct human-to-human transmission and indirect transmission via contaminated surfaces. A value of $R_0 > 1$ indicates that the monkeypox can spread and persist, while $R_0 < 1$ suggests that the monkeypox will eventually die out. This threshold informs the assessment of public health strategies such as quarantine, sanitation, and contact reduction, with the aim of reducing R_0 below one to achieve disease control.

3.2. Monkeypox Endemic Equilibrium

The monkeypox endemic equilibrium (MEE) point of system (1) refers to a state where monkeypox persists in the population. It is obtained by setting the system of equations in (1) to zero and solving for the equilibrium values of the variables.

Theorem 4. *The SEIQR-C model (1) admits a monkeypox endemic equilibrium given by* $\mathcal{E}_* = (S_*, I_*, E_*, Q_*, R_*, C_*)$.

Proof. Let $\mathcal{E}_* = (S_*, E_*, I_*, Q_*, R_*, C_*)$ be a monkeypox endemic equilibrium of the SEIQR-C model. To solve the MEE, we set all the time derivatives in the system (1) to zero. That is,

$$\begin{aligned}
\Lambda - (\beta_h I_* + \beta_c C_*)\, S_* - \mu_h S_* &= 0 \\
(\beta_h I_* + \beta_c C_*)\, S_* - (\gamma + \mu_h) E_* &= 0 \\
\gamma E_* - (\gamma_0 + \theta + \mu_h) I_* &= 0 \\
\theta I_* - (\gamma_q + \mu_h) Q_* &= 0 \\
\gamma_0 I_* + \gamma_q Q_* - \mu_h R_* &= 0 \\
\alpha I_* - \mu_p C_* &= 0.
\end{aligned}$$

Suppose that $\mathcal{E}_* = (S_*, E_*, I_*, Q_*, R_*, C_*)$ is a nontrivial equilibrium point, where all components are nonzero, indicating that the environment is not monkeypox-free. To solve for S_*, we can express the third and sixth equations in terms of I_*:

$$E_* = \frac{(\gamma_0 + \theta + \mu_h) I_*}{\gamma} \quad \text{and} \quad C_* = \frac{\alpha I_*}{\mu_p}.$$

Substituting E_* and C_* into the second equation equation and solving for S_*, we obtain

$$S_* = \frac{\mu_p(\gamma + \mu_h)(\gamma_0 + \theta + \mu_h)}{\gamma(\beta_h \mu_p + \beta_c \alpha)}. \tag{27}$$

Next, to solve for I_*, we substitute the expressions for C_* and S_* into the first equation. After algebraic manipulation, we get

$$I_* = \frac{\Lambda\gamma(\beta_h \mu_p + \beta_c \alpha) - \mu_h \mu_p (\gamma + \mu_h)(\gamma_0 + \theta + \mu_h)}{(\gamma + \mu_h)(\gamma_0 + \theta + \mu_h)(\beta_h \mu_p + \beta_c \alpha)}. \tag{28}$$

Moreover, the remaining variables E_*, Q_*, R_* and C_* are obtained by substituting I_* into the third, fourth, fifth, and sixth equations, respectively.

$$E_* = \frac{\Lambda\gamma(\beta_h \mu_p + \beta_c \alpha) - \mu_h \mu_p (\gamma + \mu_h)(\gamma_0 + \theta + \mu_h)}{\gamma(\gamma + \mu_h)(\beta_h \mu_p + \beta_c \alpha)} \tag{29}$$

$$Q_* = \frac{\Lambda\gamma\theta(\beta_h \mu_p + \beta_c \alpha) - \mu_h \mu_p \theta(\gamma + \mu_h)(\gamma_0 + \theta + \mu_h)}{(\gamma_q + \mu_h)(\gamma + \mu_h)(\gamma_0 + \theta + \mu_h)(\beta_h \mu_p + \beta_c \alpha)} \tag{30}$$

$$R_* = \frac{\gamma_0 I_* + \gamma_q Q_*}{\mu_h} \tag{31}$$

$$C_* = \frac{\Lambda\gamma\alpha(\beta_h \mu_p + \beta_c \alpha) - \mu_h \mu_p \alpha(\gamma + \mu_h)(\gamma_0 + \theta + \mu_h)}{\mu_p(\gamma + \mu_h)(\gamma_0 + \theta + \mu_h)(\beta_h \mu_p + \beta_c \alpha)} \tag{32}$$

This completes the proof. ■

Theorem 5. *If $R_0 > 1$, then the SEIQR-C model (1) has a unique positive endemic equilibrium.*

Proof. Let $R_0 > 1$. Note that $R_0 = \frac{\Lambda\gamma(\beta_h\mu_p+\alpha\beta_c)}{\mu_h\mu_p(\gamma+\mu_h)(\gamma_0+\theta+\mu_h)}$. Then,

$$S_* = \frac{\mu_p(\gamma+\mu_h)(\gamma_0+\theta+\mu_h)}{\gamma(\beta_h\mu_p+\beta_c\alpha)} = \frac{\Lambda}{\mu_h R_0} \tag{33}$$

$$E_* = \frac{\Lambda\gamma(\beta_h\mu_p+\beta_c\alpha) - \mu_h\mu_p(\gamma+\mu_h)(\gamma_0+\theta+\mu_h)}{\gamma(\gamma+\mu_h)(\beta_h\mu_p+\beta_c\alpha)} = \frac{\Lambda(R_0-1)}{(\gamma+\mu_h)R_0} \tag{34}$$

$$I_* = \frac{\Lambda\gamma(\beta_h\mu_p+\beta_c\alpha) - \mu_h\mu_p(\gamma+\mu_h)(\gamma_0+\theta+\mu_h)}{(\gamma+\mu_h)(\gamma_0+\theta+\mu_h)(\beta_h\mu_p+\beta_c\alpha)} = \frac{\Lambda\gamma(R_0-1)}{(\gamma+\mu_h)(\gamma_0+\theta+\mu_h)R_0} \tag{35}$$

$$R_* = \frac{\gamma_0 I_* + \gamma_q Q_*}{\mu_h} = \frac{(\theta R_0-1)\Lambda\gamma(\beta_h\mu_p+\beta_c\alpha)}{\gamma_q(\gamma+\mu_h)(\gamma_0+\theta+\mu_h)(\beta_h\mu_p+\beta_c\alpha)R_0} \tag{36}$$

$$C_* = \frac{\Lambda\gamma\alpha(\beta_h\mu_p+\beta_c\alpha) - \mu_h\mu_p\alpha(\gamma+\mu_h)(\gamma_0+\theta+\mu_h)}{\mu_p(\gamma+\mu_h)(\gamma_0+\theta+\mu_h)(\beta_h\mu_p+\beta_c\alpha)} = \frac{\alpha(R_0-1)\Lambda\gamma(\beta_h\mu_p+\beta_c\alpha)}{\mu_p(\gamma+\mu_h)(\gamma_0+\theta+\mu_h)(\beta_h\mu_p+\beta_c\alpha)R_0} \tag{37}$$

Hence, the unique positive endemic equilibrium of the SEIQR-C model (1) exists when $R_0 > 1$. ■

3.3. Stability Analysis

This section presents the local stability analysis of the equilibrium points of the SEIQR-C model for monkeypox.

Theorem 6. *If $R_0 < 1$, then the SEIQR-C model (1) is locally asymptotically stable at the monkeypox-free equilibrium $\mathcal{E}_0$ and unstable otherwise.*

Proof. The Jacobian matrix of the system (1) is given by

$$J = \begin{bmatrix} -(\beta_h I+\beta_c C)-\mu_h & 0 & -\beta_h S & 0 & 0 & -\beta_c S \\ \beta_h I+\beta_c C & -(\gamma+\mu_h) & \beta_h S & 0 & 0 & \beta_c S \\ 0 & \gamma & -(\gamma_0+\theta+\mu_h) & 0 & 0 & 0 \\ 0 & 0 & \theta & -(\gamma_q+\mu_h) & 0 & 0 \\ 0 & 0 & \gamma_0 & \gamma_q & -\mu_h & 0 \\ 0 & 0 & \alpha & 0 & 0 & -\mu_p \end{bmatrix}. \tag{38}$$

The Jacobian matrix evaluated at $\mathcal{E}_0$ is of the form

$$J_{\mathcal{E}_0} = \begin{bmatrix} -\mu_h & 0 & \frac{-\beta_h\Lambda}{\mu_h} & 0 & 0 & \frac{-\beta_c\Lambda}{\mu_h} \\ 0 & -(\gamma+\mu_h) & \frac{\beta_h\Lambda}{\mu_h} & 0 & 0 & \frac{\beta_h\Lambda}{\mu_h} \\ 0 & \gamma & -(\gamma_0+\theta+\mu_h) & 0 & 0 & 0 \\ 0 & 0 & \theta & -(\gamma_q+\mu_h) & 0 & 0 \\ 0 & 0 & \gamma_0 & \gamma_q & -\mu_h & 0 \\ 0 & 0 & \alpha & 0 & 0 & -\mu_p \end{bmatrix}. \tag{39}$$

Then, the first four eigenvalues obtained are $\lambda_1 = -\mu_h$, $\lambda_2 = -\mu_p$, $\lambda_3 = -\mu_h$, and $\lambda_4 = -(\gamma_q + \mu_h)$, while the remaining two eigenvalues can be determined as the roots of the following second-degree polynomial:

$$\lambda^2 + (\gamma + 2\mu_h + \gamma_0 + \theta)\lambda + (\gamma + \mu_h)(\gamma_0 + \theta + \mu_h) - \frac{\Lambda\gamma\beta_h}{\mu_h}.$$

Suppose $R_0 < 1$. Then R_0 can be express as

$$\frac{\Lambda\gamma\beta_h\mu_p}{\mu_h\mu_p(\gamma + \mu_h)(\gamma_0 + \theta + \mu_h)} + \frac{\Lambda\gamma\alpha\beta_c}{\mu_h\mu_p(\gamma + \mu_h)(\gamma_0 + \theta + \mu_h)} < 1.$$

It follows that,

$$\frac{\Lambda\gamma\beta_h}{\mu_h(\gamma + \mu_h)(\gamma_0 + \theta + \mu_h)} < 1.$$

Multiply both sides by $(\gamma + \mu_h)(\gamma_0 + \theta + \mu_h)$, we have

$$\frac{\Lambda\gamma\beta_h}{\mu_h} < (\gamma + \mu_h)(\gamma_0 + \theta + \mu_h).$$

Subsequently,

$$(\gamma + \mu_h)(\gamma_0 + \theta + \mu_h) - \frac{\Lambda\gamma\beta_h}{\mu_h} > 0.$$

By Routh-Hurwitz criterion [23], all eigenvalues of the second-degree polynomial are negative when $R_0 < 1$. Thus, the SEIQR-C model (1) is locally asymptotically stable at the monkeypox-free equilibrium $\mathcal{E}_0$ when $R_0 < 1$ and unstable otherwise. ■

Theorem 7. *If $R_0 < 1$, then the SEIQR-C model (1) is globally asymptotically stable at the monkeypox-free equilibrium $\mathcal{E}_0$ and unstable otherwise.*

Proof. Consider the Lyapunov function below

$$\mathcal{L} = E + \frac{\gamma + \mu_h}{\gamma} I + \frac{\Lambda\beta_c}{\mu_h\mu_p} C.$$

The time derivative of $\mathcal{L}$ calculated along the solution of the system (1) is negative definite. That is,

$$\frac{d\mathcal{L}}{dt} = \frac{dE}{dt} + \left(\frac{\gamma + \mu_h}{\gamma}\right)\frac{dI}{dt} + \left(\frac{\Lambda\beta_c}{\mu_h\mu_p}\right)\frac{dC}{dt} \tag{40}$$

$$= \beta_h SI + \beta_c SC - (\gamma + \mu_h)E + \Big(\frac{\gamma + \mu_h}{\gamma}\Big)\Big(\gamma E - (\gamma_0 + \theta + \mu_h)I\Big) + \frac{\alpha\beta_c}{\mu_h\mu_p}\Big(\alpha I - \mu_p C\Big) \tag{41}$$

$$= \beta_h SI + \Big(\frac{\gamma+\mu_h}{\gamma}\Big)\Big(-(\gamma_0+\theta+\mu_h)I\Big) + \frac{\alpha\beta_c\alpha}{\mu_h\mu_p}I \tag{42}$$

$$= \left(\frac{\beta_h\Lambda}{\mu_h} + \frac{\Lambda\beta_h\alpha}{\mu_h\mu_p} - \frac{(\gamma+\mu_h)(\gamma_0+\theta+\mu_h)}{\gamma}\right)I \tag{43}$$

$$= \left(\frac{\mu_p\beta_h\Lambda + \Lambda\beta_h\alpha}{\mu_h\mu_p} - \frac{(\gamma+\mu_h)(\gamma_0+\theta+\mu_h)}{\gamma}\right)I \tag{44}$$

$$= \frac{(\gamma+\mu_h)(\gamma_0+\theta+\mu_h)}{\gamma}\Big(R_0-1\Big)I \tag{45}$$

$$\leq 0 \quad \text{for} \quad R_0 < 1. \tag{46}$$

The time derivative $\frac{d\mathcal{L}}{dt} \leq 0$ whenever the basic reproduction number $R_0 < 1$. The equality $\frac{d\mathcal{L}}{dt} = 0$ holds only when $E = I = C = 0$, that is, at the monkeypox-free equilibrium $\mathcal{E}_0$. Therefore, by LaSalle's Invariance Principle [24], it follows that the largest positively invariant set where $\frac{d\mathcal{L}}{dt} = 0$ is the singleton $\mathcal{E}_0$, and thus all solutions in Ω converge to $\mathcal{E}_0$. This establishes that the monkey-free equilibrium of the SEIQR-C model is globally asymptotically stable whenever $R_0 < 1$. ■

3.4. Sensitivity Analysis

The sensitivity index quantifies the relative change in R_0 in response to a relative change in a parameter [25]. Given the basic reproduction number for the SEIQR-C model (1)

$$R_0 = \frac{\Lambda\gamma(\beta_h\mu_p + \alpha\beta_c)}{\mu_h\mu_p(\gamma+\mu_h)(\gamma_0+\theta+\mu_h)} \tag{47}$$

the sensitivity index of R_0 with respect to a parameter p is defined as

$$S_p = \frac{\partial R_0}{\partial p}\cdot\frac{p}{R_0}. \tag{48}$$

The sensitivity index for each parameter of the SEIQR-C model (1) with respect to R_0 is given by:

$$S_\Lambda = \frac{\partial R_0}{\partial \Lambda}\cdot\frac{\Lambda}{R_0} = 1 \tag{49}$$

$$S_\gamma = \frac{\partial R_0}{\partial \gamma}\cdot\frac{\gamma}{R_0} = R_0\left(\frac{1}{\gamma} - \frac{1}{\gamma+\mu_h}\right)\cdot\frac{\gamma}{R_0} = \frac{\mu_h}{\gamma+\mu_h} \tag{50}$$

$$S_{\beta_h} = \frac{\partial R_0}{\partial \beta_h}\cdot\frac{\beta_h}{R_0} = \frac{\beta_h\mu_p}{\beta_h\mu_p + \alpha\beta_c} \tag{51}$$

$$S_{\beta_c} = \frac{\partial R_0}{\partial \beta_c}\cdot\frac{\beta_c}{R_0} = \frac{\alpha\beta_c}{\beta_h\mu_p + \alpha\beta_c} \tag{52}$$

$$S_\alpha = \frac{\partial R_0}{\partial \alpha}\cdot\frac{\alpha}{R_0} = \frac{\alpha\beta_c}{\beta_h\mu_p + \alpha\beta_c} \tag{53}$$

$$S_{\mu_p} = \frac{\partial R_0}{\partial \mu_p} \cdot \frac{\mu_p}{R_0} = -\frac{\alpha\beta_c}{\beta_h\mu_p + \alpha\beta_c} \tag{54}$$

$$S_{\mu_h} = \frac{\partial R_0}{\partial \mu_h} \cdot \frac{\mu_h}{R_0} = -1 - \frac{\mu_h(\gamma + \gamma_0 + \theta + 2\mu_h)}{(\gamma + \mu_h)(\gamma_0 + \theta + \mu_h)} \tag{55}$$

$$S_{\gamma_0} = \frac{\partial R_0}{\partial \gamma_0} \cdot \frac{\gamma_0}{R_0} = -\frac{\gamma_0}{\gamma_0 + \theta + \mu_h} \tag{56}$$

$$S_{\theta} = \frac{\partial R_0}{\partial \theta} \cdot \frac{\theta}{R_0} = -\frac{\theta}{\gamma_0 + \theta + \mu_h}. \tag{57}$$

$$\tag{58}$$

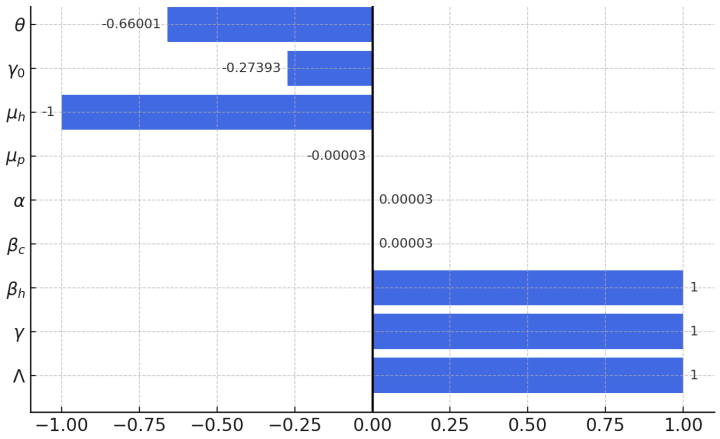

Figure 2: Sensitivity indices of the SEIQR-C model parameters

Figure 2 presents the sensitivity indices of the SEIQR-C model. The results reveal that the recruitment rate (Λ), the human-to-human transmission rate (β_h), the progression rate from exposed to infectious individuals (γ), the transmission rate from contaminated surfaces (β_c), and the contamination rate (α) exhibit a positive impact on the basic reproduction number (R_0). This indicates that increases in these parameters contribute to a higher potential for monkeypox transmission. Conversely, the cleaning or decay rate (μ_p), the natural death rate (μ_h), the recovery rate (γ_0), and the quarantine rate (θ) show negative sensitivity indices. This suggests that increasing these parameters effectively reduces R_0, leading to a decrease in the number of individuals infected with monkeypox.

4. Simulation

In this section, we present numerical simulations to illustrate the theoretical findings. The parameter values used in the simulations are listed in Table 1.

Simulation 1. The parameter values utilized in this study are presented in Table 1. Using these parameters, we compute the basic reproduction number as $R_0 = 0.917$, and determine the monkeypox-free equilibrium to be $\mathcal{E}_0 = (25, 0, 0, 0, 0, 0)$. The initial

conditions for the compartments of the SEIQR-C model are considered as follows: (a) $(100, 70, 50, 40, 30, 55)$, (b) $(200, 130, 90, 100, 90, 130)$, (c) $(500, 300, 190, 150, 125, 220)$, and (d) $(1000, 565, 455, 225, 155, 350)$. As shown in Figure 3, for all initial conditions, the solution trajectories converge to the monkeypox-free equilibrium $\mathcal{E}_0 = (25, 0, 0, 0, 0, 0)$. This result indicates that the SEIQR-C model exhibits local asymptotic stability at the monkeypox-free equilibrium when $R_0 < 1$.

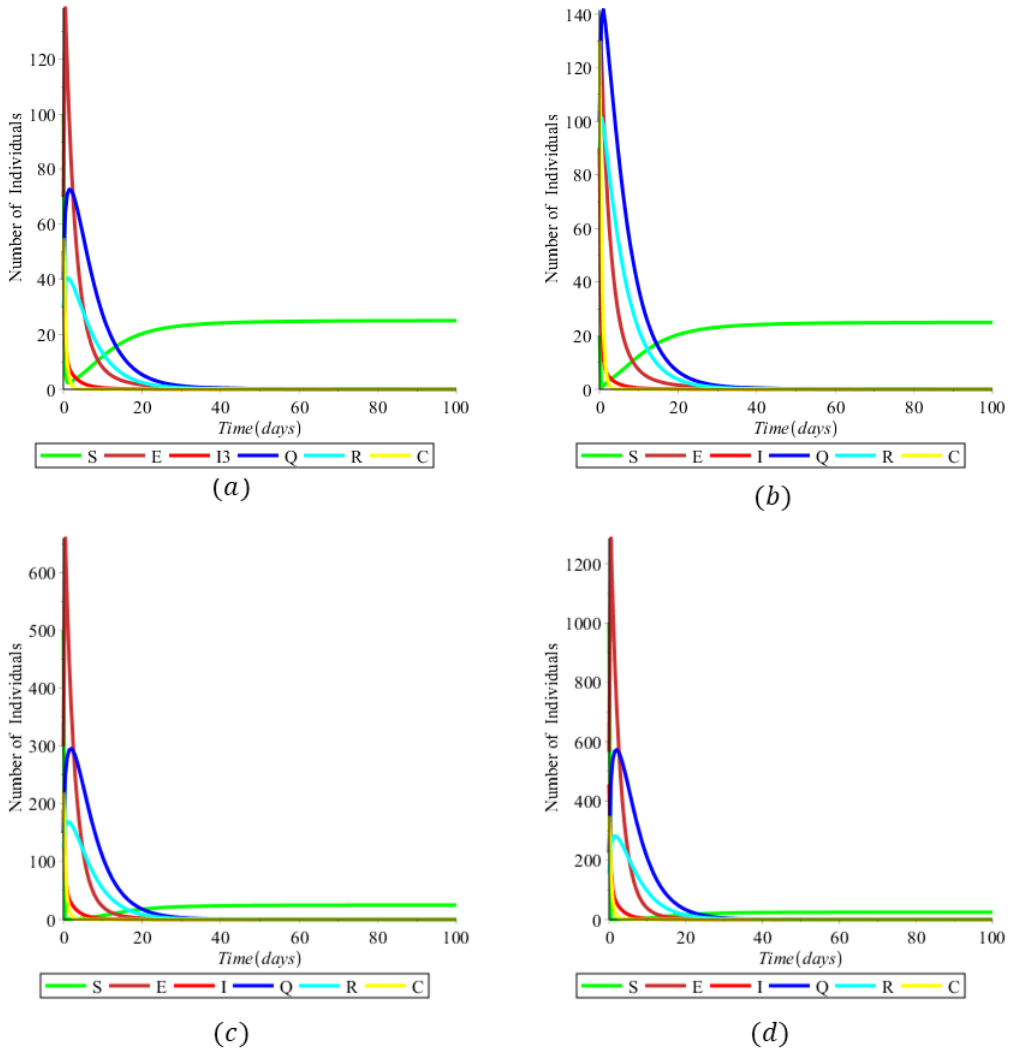

Figure 3: (Simulation 1) The SEIRQ-C model is locally asymptotically stable at $\mathcal{E}_0$ when $R_0 < 1$.

Simulation 2. Consider the same parameter values used in Simulation 1, except for an increased recruitment rate of $\Lambda = 10$, and decreased values of the quarantine rate $\theta = 0.5$ and the cleaning or decay rate $\mu_p = 0.3$. As a result, the basic reproduction

number increases to $R_0 = 21.786$, while the disease-free equilibrium remains at $\mathcal{E}_0 = (25, 0, 0, 0, 0, 0)$. Using the same initial conditions as in Simulation 1, it is observed from Figure 4 that the solution trajectories do not converge to $\mathcal{E}_0$, indicating that the SEIQR-C model is unstable at the disease-free equilibrium when $R_0 > 1$. Furthermore, since $R_0 = 21.786$ and the endemic equilibrium point $\mathcal{E}_* = (15, 18, 4, 6, 9, 1)$ now exists, the solution trajectories are seen to converge to $\mathcal{E}_*$. Therefore, the SEIQR-C model is locally asymptotically stable at the endemic equilibrium whenever $R_0 > 1$.

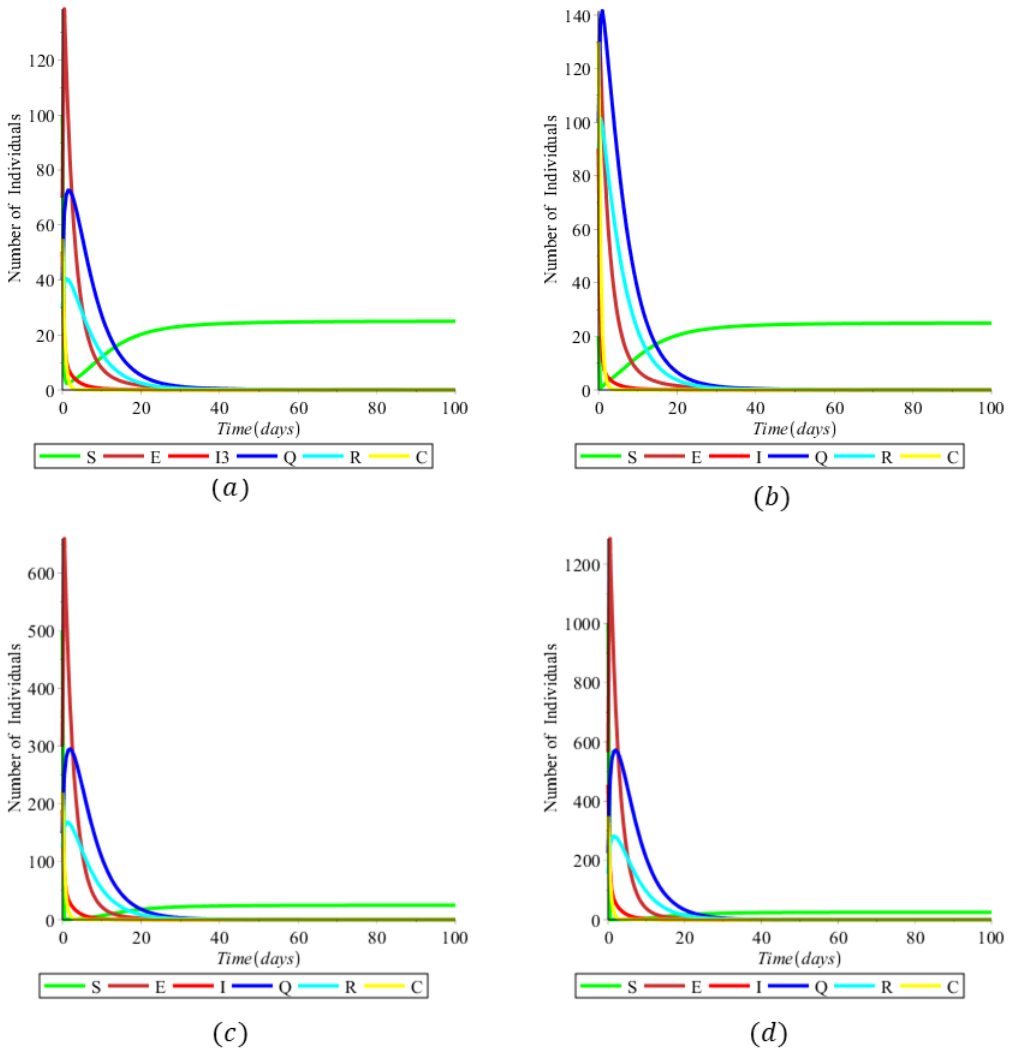

Figure 4: (Simulation 2) The SEIRQ-C model is locally asymptotically stable at $\mathcal{E}_*$ when $R_0 > 1$.

Figures 3 and 4 further demonstrate the contrasting epidemic dynamics of the SEIQR-C model under varying control parameters while maintaining identical initial values for

all compartments. In Figure 3 ($R_0 < 1$), higher quarantine (θ) and cleaning or viral decay rate (μ_p) lead to a progressive reduction in the number of infectious individuals and environmental contamination, confirming the stability of the disease-free equilibrium. Conversely, in Figure 4 ($R_0 > 1$), the same initial conditions are applied but with lower values of θ and μ_p, resulting in persistent infection and convergence toward an endemic equilibrium. These findings highlight that the effectiveness of quarantine measures and environmental sanitation plays a critical role in reducing the basic reproduction number and ensuring the long-term stability of the human population against monkeypox transmission. Although no previous model has simultaneously incorporated quarantine and contaminated surfaces, the present results are comparable to those in [15] and [16], which also emphasized the importance of quarantine and environmental sanitation in controlling the spread of monkeypox.

5. Conclusion

This study formulated and analyzed a deterministic SEIQR-C model to describe the transmission dynamics of monkeypox by incorporating both quarantine protocols and environmental contamination. The model ensured non-negative and bounded solutions, and equilibrium analyses identified both disease-free and endemic states. Stability analyses demonstrated that the disease-free equilibrium is locally and globally asymptotically stable when $R_0 < 1$, while the endemic equilibrium becomes locally stable when $R_0 > 1$. Numerical simulations further validated these theoretical findings, showing that the infection dies out when quarantine and cleaning measures are adequately implemented. The results emphasize that increasing the efficiency of quarantine and the rate of surface cleaning or viral decay are among the most effective strategies for controlling monkeypox transmission, particularly in low-resource settings where vaccine coverage remains limited.

While the SEIQR-C model provides valuable insights into the combined effects of quarantine and surface contamination, it is based on several simplifying assumptions. The current model does not include vaccination dynamics, disease-induced mortality, or parameter estimation using real outbreak data. Furthermore, the global stability of the endemic equilibrium was not established. Future studies may focus on constructing a Lyapunov function to determine the global stability of the endemic equilibrium, extending the model to incorporate disease-induced mortality and vaccination, and validating the model through real-data fitting and parameter estimation. These directions will enhance the model's applicability and improve its predictive capability for guiding public health policies against monkeypox transmission.

Conflict of Interest

The author affirms that no conflict of interest exists with respect to the research, authorship, and/or publication of this article.

Acknowledgments

The author would like to thank all individuals and institutions who supported the completion of this study.

References

[1] World Health Organization. Monkeypox, 04 2023.

[2] Eveline Bunge, Bernard Hoet, Liddy Chen, Florian Lienert, Heinz Weidenthaler, L. R. Baer, and Robert Steffen. The changing epidemiology of human monkeypox—a potential threat? a systematic review. *PLOS Neglected Tropical Diseases*, 16:e0010141, 02 2022.

[3] Z. Jezek and F. Fenner. Human monkeypox. *Karger Publishers*, 17, 10 1988.

[4] World Health Organization. Disease outbreak news, 2023.

[5] S. A. Boone and C. P. Gerba. Significance of fomites in the spread of respiratory and enteric viral disease. *Applied and Environmental Microbiology*, 73:1687–1696, 01 2007.

[6] L. D. Nolen, J. Osadebe, Katomba, J. Likofata, D. Mukadi, B. Monroe, J. Doty, C. M. Hughes, J. Kabamba, J. Malekani, P. L. Bomponda, J. I. Lokota, M. P. Balilo, T. Likafi, R. S. Lushima, B. K. Ilunga, F. Nkawa, E. Pukuta, S. Karhemere, J. J. M. Tamfum, B. Nguete, E. O. Wemakoy, A. McCollum, and M. Reynolds. Extended human-to-human transmission during a monkeypox outbreak in the democratic republic of the congo. *Emerging Infectious Diseases*, 22:1014–1021, 06 2016.

[7] A. Yinka-Ogunleye, O. Aruna, D. Ogoina, N. Aworabhi, W. Eteng, S. Badaru, A. Mohammed, J. Agenyi, E. N. Etebu, T. W. Numbere, A. Ndoreraho, E. Nkunzimana, Y. Disu, M. Dalhat, P. Nguku, A. Mohammed, M. Saleh, A. McCollum, K. Wilkins, O. Faye, A. Sall, C. Happi, N. Mba, O. Ojo, and C. Ihekweazu. Reemergence of human monkeypox in nigeria, 2017. *Emerging Infectious Diseases*, 24(6), 06 2018.

[8] C. Morgan, F. Whitehill, J. Doty, J. Schulte, A. Matheny, J. Stringer, L. Delaney, R. Esparza, A. Rao, and A. McCollum. Environmental persistence of monkeypox virus on surfaces in household of person with travel-associated infection, dallas, texas, usa, 2021. *Emerging Infectious Diseases*, 28, 10 2022.

[9] D. Nörz, S. Pfefferle, T. Brehm, G. Franke, I. Grewe, B. Knobling, M. Aepfelbacher, S. Huber, E. Klupp, S. Jordan, M. Addo, J. Schulze zur Wiesch, S. Schmiedel, M. Lütgehetmann, and J. Knobloch. Evidence of surface contamination in hospital rooms occupied by patients infected with monkeypox, germany, june 2022. *Eurosurveillance*, 27, 06 2022.

[10] M. Christodoulidou and N. Mabbott. Efficacy of smallpox vaccines against mpox infections in humans. *Immunotherapy Advances*, 3, 10 2023.

[11] A. Hossain, Md. A. Monem, M. Rahman, and R. Raza. Mpox (monkeypox): a comprehensive update of current epidemic evidence. *Science in One Health*, 4:100100, 12 2024.

[12] E. Roxas, P. J. Acacio-Claro, M. M. Lota, A. Abeleda, S. N. Dalisay, M. Landicho,

Y. Fujimori, J. Z. Rosuello, J. Kaufman, M. Danchin, V. Belizario, and F. Vogt. Enablers and barriers of covid-19 vaccination in the philippines. *Vaccines*, 13:719–719, 07 2025.

[13] M. Ngungu, E. Addai, A. Adeniji, A. Umar Muhammad, and Kayode O. Mathematical epidemiological modeling and analysis of monkeypox dynamism with non-pharmaceutical intervention using real data from united kingdom. *Frontiers in Public Health*, 11, 02 2023.

[14] J. Puebla, J. M. Macalalag, and K. Pajaron. A mathematical model for covid-19 and tuberculosis coinfection with the effect of a quarantine measure. *European Journal of Pure and Applied Mathematics*, 18:6149–6149, 08 2025.

[15] B. Bolaji, A. Ibrahim, F. Ani, B. Omede, and G. Acheneje. A model for the control of transmission dynamics of human monkeypox disease in sub-saharan africa. *Journal of the Nigerian Society of Physical Sciences*, pages 1800–1800, 05 2024.

[16] A. Hassan, A. Dipo, and Muhamad. Optimal control and stability analysis of monkeypox transmission dynamics with the impact of contaminated surfaces. *Frontiers in Applied Mathematics and Statistics*, 10, 03 2024.

[17] A. Alshehri and S. Ullah. Optimal control analysis of monkeypox disease with the impact of environmental transmission. *AIMS Mathematics*, 8:16926–16960, 01 2023.

[18] O. J. Peter, S. Kumar, N. Kumari, F. A. Oguntolu, K. Oshinubi, and R. Musa. Transmission dynamics of monkeypox virus: a mathematical modelling approach. *Modeling Earth Systems and Environment*, 10 2021.

[19] C. Madubueze, I. Onwubuya, G. Nkem, and Z. Chazuka. The transmission dynamics of the monkeypox virus in the presence of environmental transmission. *Frontiers in Applied Mathematics and Statistics*, 8, 11 2022.

[20] O. Diekmann, J. A. P. Heesterbeek, and J. A. J. Metz. On the definition and the computation of the basic reproduction ratio r 0 in models for infectious diseases in heterogeneous populations. *Journal of Mathematical Biology*, 28, 06 1990.

[21] V. D. Driessche and J. Watmough. Reproduction numbers and sub-threshold endemic equilibria for compartmental models of disease transmission. *Mathematical Biosciences*, 180:29–48, 11 2002.

[22] C. Castillo-Chávez, Z. Feng, W. Huang, P. Driessche, D. Kirschner, and Y. Abdul-Aziz. On the computation of r0 and its role in global stability, 01 2022.

[23] T. Roskilly and R. Mikalsen. *Marine systems identification, modeling and control*. Elsevier/Bh, Butterworth-Heinemann Is An Imprint Of Elsevier, 2015.

[24] J. P. LaSalle. *The Stability of Dynamical Systems*. SIAM, 01 1976.

[25] M. Martcheva. *An Introduction to Mathematical Epidemiology*. Springer US, 2015.